Micromachining with a High Repetition Rate Femtosecond Fiber Laser

Fumiyo YOSHINO*, Lawrence SHAH**, Martin FERMANN**, Alan ARAI*, Yuzuru UEHARA**

*IMRA America, Inc., Applications Research Laboratory
48834 Kato Road, Suite 106A, Fremont, CA 94538 U.S.A.
E-mail: fyoshino@imra.com
** IMRA America, Inc.
1044 Woodridge Avenue, Ann Arbor, Michigan 48105 U.S.A.

Industrial micromachining applications with ultrashort pulse lasers are often difficult to make practical due to the lack of robustness of the laser and the slow processing speed resulting from the low repetition rate. In the past, amplified, femtosecond lasers produced high pulse energies, but at a slow pulse repetition rate of around a kHz. The high repetition rate oscillators did not have enough pulse energy for micromachining of most industrial materials.

Fiber Chirped Pulse Amplification (FCPA) is bridging these two performance regimes, producing relatively high pulse energies (compared to oscillators) and relatively high repetition rates (compared to amplifiers) in a robust and reliable package. The FCPA *μJewel* D-1000 has a flexible performance range that includes 10-μJ pulses at 100 kHz and 1-μJ pulses at 1 MHz.

The μJ pulses at MHz repetition rates enable some interesting micromachining processes, particularly with transparent dielectric materials where thermal accumulation begins to play an important role in the process. This paper expands on previously reported work on micromachining of transparent materials using a high repetition rate, femtosecond fiber laser.

DOI: 10.2961/jlmn.2008.03.0006

Keywords: femtosecond, ultrafast, micromachining, sapphire, glass, laser scribing

1. Introduction

Micromachining of transparent materials with ultrashort pulse lasers has the capability of unique material processing such as 3D modifications in transparent materials via nonlinear absorption [1]. Applications include optical waveguide writing, nano/micro-channel fabrication in bulk, and direct welding without additive materials [2,3,4].

Despite the fact that extensive research on femtosecond laser technologies has been conducted over the years, ultrashort pulse lasers have not yet been widely used in the industrial environment largely due to the lack of suitable systems.

IMRA's FCPA *μJewel* system offers a high energy and a high repetition rate combination which is essential for fast processing required for industrial manufacturing.

The advantage of higher repetition rates for some applications, such as optical waveguide writing [2,5] and transparent material welding [4,6], was demonstrated using the 2-μJ FCPA *μJewel* D-400 system.

Our latest system, the FCPA *μJewel* D-1000, offers higher average power compared to the D-400, with the same variable repetition rate from 100 kHz to 5 MHz. The highest pulse energy available is 10 μJ at the lowest repetition rate 100 kHz. IMRA accumulated experience has produced a reliable, robust laser, with units exceeding 17,000 hours of operation. Figure 1 shows a photo of the laser head and controller. The laser head has dimensions of 550x400x131 mm^3 and weighs about 30 kg.

In this paper, we discuss the effects of different laser processing conditions available from the FCPA *μJewel* D-1000 for several interesting applications and industrially important transparent materials.

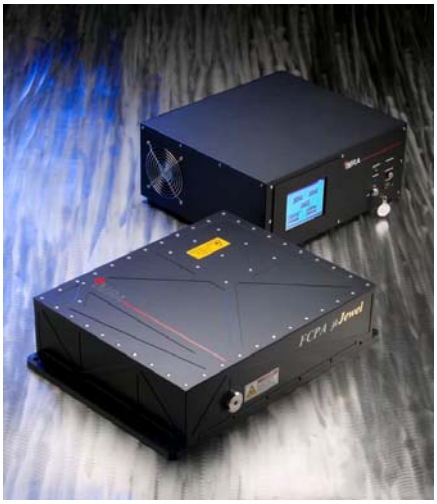

Fig. 1 FCPA *μJewel* D-1000 laser head & controller.

2. Sub-Surface Modification of Transparent Materials

One of the advantages of using a high repetition rate with high average power is that thermal accumulation in the target materials occurs more readily. This was demonstrated for optical waveguide writing in glass with lower pulse energy using the FCPA *μJewel* D-400 system [5]. Much higher repetition rate, 10s of MHz, has been studied for waveguide writing in various materials [7]. Transparent material melting by femtosecond pulses can be used as an effective method for welding 2 pieces of glass or 2 different materials [8]. In order to see the advantage of high repetition rate and high average power for this application,

we have tested melting of fused silica (Corning 7980) and borosilicate glass (Schott D263). These two types of glass are significantly different in material properties and their response to laser processing.

2.1 Borosilicate Glass (Schott D263)

Previously, high repetition rate ultrashort pulses were studied through experiments with lower pulse energy and through computer simulation [6]. At the high repetition rate, more pulses interact with a particular volume of material. The initial pulses increase the absorptivity of the material for the subsequent pulses rapidly elevating the temperature. With the FCPA *μJewel* D-1000, we can study similar repetition rates, but with higher pulse energy, to see the effect on glass melting.

When the pulse energy and the pulse overlap were kept the same, the higher repetition rate showed larger melt region as was reported previously [5].

In these experiments, the average power was kept the same for all repetition rates. A 60x aspheric lens was used as the focusing objective. Scan speeds were 20~80 mm/s.

At all the test conditions, melting was observed (Figure 2). With 1 W average power, the size of the melt did not change dramatically at repetition rates below 1 MHz.

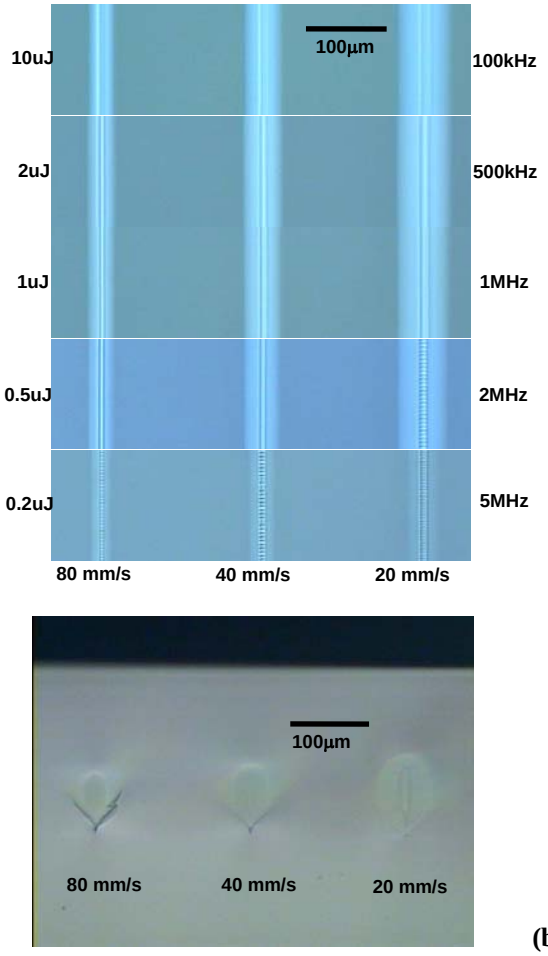

Fig. 2 Melt region in D263 with various process conditions (laser: 100 kHz, 10μJ, 1W) **(a)** top and **(b)** cross-sectional view (laser focused from above)

However, above 1 MHz there is a rapid reduction in the size of the melt region, particularly at lower translation speeds (Figure 3). This indicates that there is insufficient heat accumulation from nonlinear absorption to couple more laser energy into the glass and create a larger melt width.

Note that the pulse energy decreases as the repetition rate gets higher (constant average power), so the trend in Figure 3 does not follow the change of pulse energy with repetition rate. This is likely to contribute to the smaller melt width. However, the change in melt width is not proportional to the change in pulse energy.

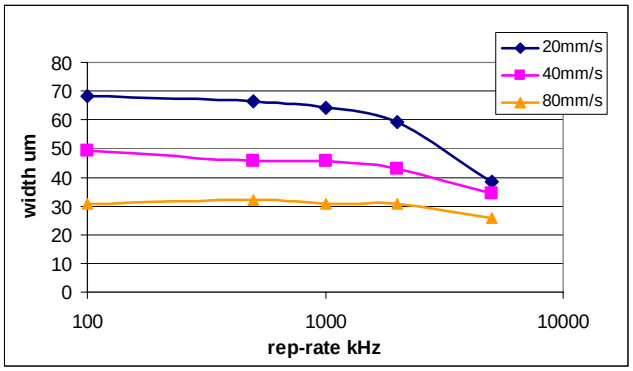

Fig. 3 D263 melt width as function of repetition rate (laser: 1W)

2.2 Fused Silica (Corning 7980)

Using the combination of a higher pulse energy with a modest repetition rate, a melt region significantly larger than focal volume (more than 14x) was demonstrated at high process speed. Scan speeds tested were 0.1 ~ 5 mm/s, 5 ~ 200 mm/s. Both 30x and 40x aspheric lenses (NA 0.37, NA 0.49, respectively) were used. However, the 40x always produced a larger melt region. Figure 4 shows the top view of the melt region for a range of repetition rates.

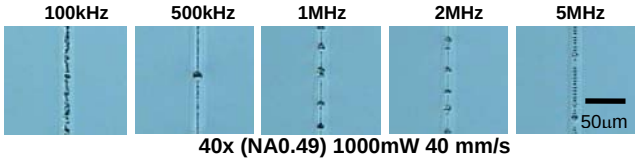

Fig. 4 Fused silica melt region at various process conditions (top view).

At 100 kHz the core part of the modified area starts to get rougher, suggesting strong ablation. The modified areas were accompanied by periodic voids, similar to those observed by other researchers [7]. The void frequency decreases with lower repetition rate and faster scan speed, however, it was not possible to eliminate them in the range of conditions tested. Nevertheless, large volume melting is possible at high scan speeds - 10s of mm/s for both fused silica and borosilicate glass.

The melt region widths are plotted in Figure 5 for the speed range of 0.1-5 mm/s at 1-5 MHz. The melt widths are larger than 20 μm, much larger than the focus diameter of 1.4 μm, which suggests heat accumulation is playing a key role. Within this range of repetition rate, the highest pulse energy at the lowest repetition rate, 1 MHz, demonstrated the largest melt volume. The melt region gets smaller with faster scan speed. At each scan speeds, the lower repetition rate and higher energy generates a larger

melt region than the higher repetition rate, low energy case (for the same average power) due to insufficient heat accumulation.

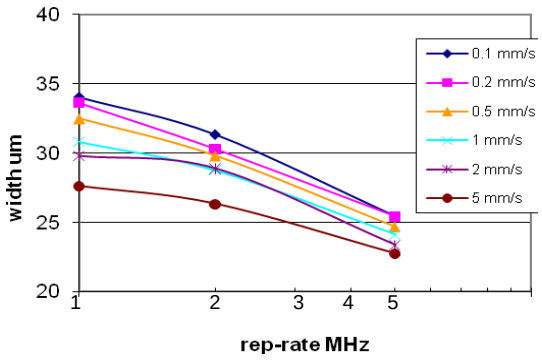

Fig. 5 Fused silica melt width as function of repetition rate

3. Multi-Scribe

We have previously demonstrated the "dual scribe" technique for scribing transparent materials in a scribe-and-break process utilizing higher pulse energy from a 50 kHz-10 μJ prototype system [9,10].

In the dual scribe process, a surface scribe line is created simultaneously with a sub-surface modified region. This second layer of modification makes the breaking process more consistent and a smoother cleave surface with a shallower surface cut. Also the dual scribe allows faster process speed than surface scribe only due to the ease of breaking.

In the dual scribe process, the beam focus is positioned below the surface of the target (Figure 6). The local fluence of the beam at the surface is still high enough to cause ablation at the center of the beam. The low-fluence portion of the beam that is not blocked by the surface ablation passes into the target material and is concentrated at the focal point of the objective. The fluence at the focal point is high enough to simultaneously create a region of modification.

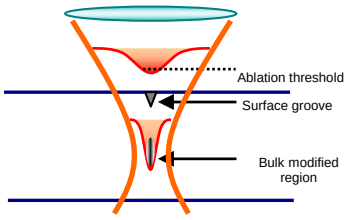

Fig. 6 Schematic of in dual scribe process [9]

Another process that contributes to the dual scribe is the formation of multiple foci and filamentation within the target material to create an elongated region of material modification along the beam axis [11,12]. The multiple foci can create "multi-scribe" containing more than one inner modification layers.

3.1 Borosilicate Glass (Corning 1737)

To investigate the multi-scribe process, first we looked at the inner material modification at various focusing conditions (NAs from 0.16 ~ 0.49) and energies. Figure 7 shows cross-section of the inner modification with NAs 0.22, 0.3, 0.37.

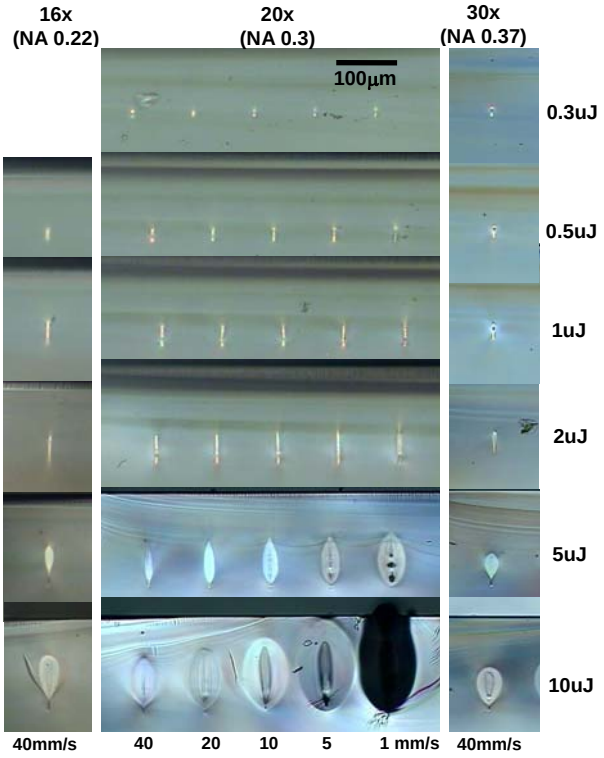

Fig. 7 Cross-sectional images of 1737 inner modification (laser beam focused from above)

Above ~5 μJ of pulse energy, the thermal accumulation starts to play a significant role in the material modification, resulting in a much wider melt region. The modified area is far larger than focal volume and it changes rapidly with scan speed. Note that as the scan speed decreases (equivalent to increasing the number of pulses), the modified region grows towards the surface and does not extend deeper into the target.

For pulse energies less than 5 μJ, the shape of the material modification does not change much with translation speed (equivalent to the number of pulses), suggesting that thermal accumulation plays less of a role for these conditions.

When comparing the different NAs shown for a translation speed of 40 mm/s, the shape of the material modification changes from "thin" to "wide" at lower pulse energy with the higher NA, indicating that the thermal accumulation effect is initiated at lower pulse energy.

The length of modified area is plotted as function of energy with different focusing optics (Figure 8a). The length of modification does not change between NA 0.22 and NA 0.3.

Figure 8b shows a significant change in the size of the focal volume that is above the damage threshold for the different NAs. A similar effect is shown by Wu [10] and is attributed to the formation of multiple foci and filamentation. In the case of 1737, distinct foci are not visible, but seem to merge into a line in this cross-sectional view.

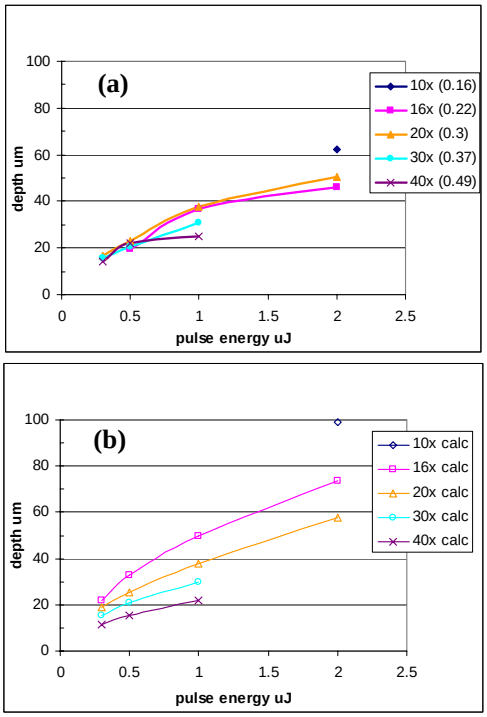

Fig. 8 Modified length vs pulse energy of 1737
(a) experimental (b) calculated

Next, the focus depth was gradually changed to monitor the onset of the multi-scribe process (Figure 9). This should also show how the multi-focus effect plays a role in multi-scribe.

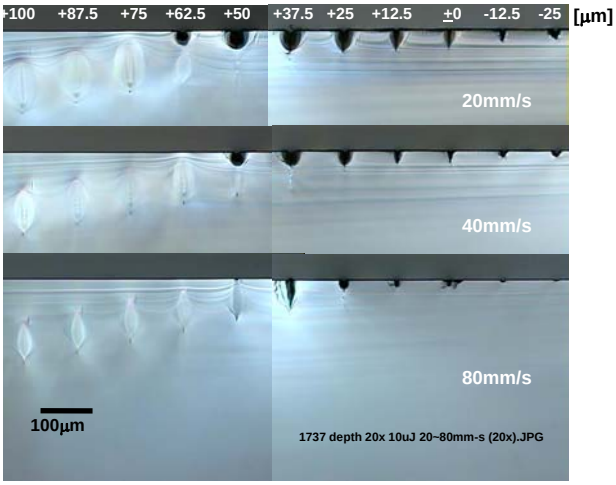

Fig. 9 Cross-sectional images of 1737 modified area with various focus depth locations (White numbers at the top, in µm, indicate the focus position with respect to the surface)

These images can be separated into 3 regions in terms of material modification. On the right side (shallowest focus positions), there are surface scribe lines only. On the left side (deepest focus locations), only inner material modifications was produced. In the middle of these two regions, there are both surface scribe lines and inner modification. This is the multi-scribe region.

The material modification, in general, is stronger at slower speeds due to higher pulse overlap. However, in the multi-scribe region, at the same focus positions the inner modification becomes stronger at higher scan speed since the surface scribe line is smaller, blocking less light into the bulk of the material.

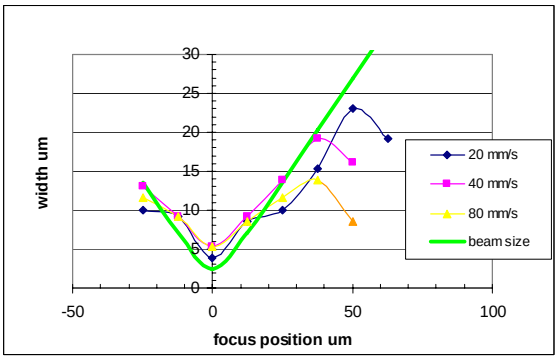

Fig. 10 Width of surface scribe line in 1737 as function of focus depth (20x aspheric lens)

Figure 9 shows that as the focus location moves deeper into the material, the surface scribe line initially becomes deep, but then reverses and become shallower (most noticeable at 20 mm/s). As the surface scribe line becomes shallower, the inner modification starts to appear. When surface scribe line completely disappears, the inner modification becomes full length and does not change. This transition region is where the multi-scribe exists.

The same observation can be drawn from the width of surface scribe shown in Figure 10. The onset of the multi-scribe process occurs near the focus depth where the beam diameter at surface starts to become larger than the surface scribe line. Figure 11 shows a successful multi-scribe at 80 mm/s.

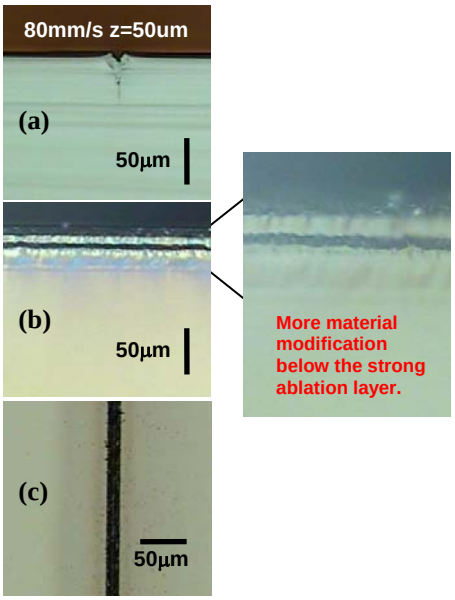

Fig. 11 Multi-scribe process of 1737
(a) cross-section, (b) cleave facet (c) top view

The sample with only a surface scribe line produced at the same scan speed did not break cleanly along the scribe line, illustrating the advantage of the multi-scribe process.

3.2 Sapphire

Similar characteristics were observed with the modification of sapphire (Figure 12). For the 16x to 20x objectives, there is almost no difference in the lengths of modifications.

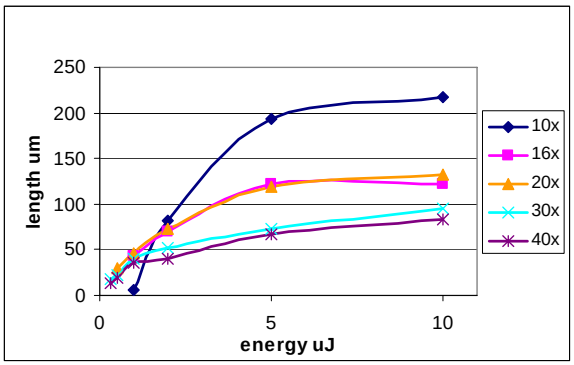

Fig. 12 Sapphire modified length vs pulse energy

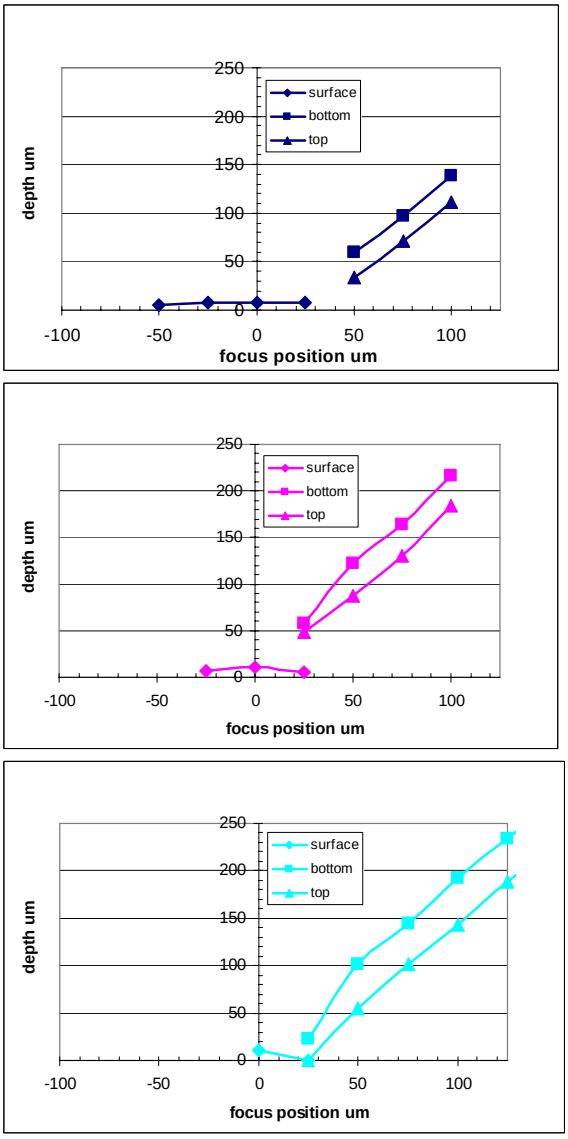

Fig. 13 Sapphire depth of modification (80 mm/s) (16, 20, 40x aspheric lens)

Figure 13 show the depths of the features for different focus positions and focusing objectives at a scan speed 80 mm/s. On the left side of the graphs (smaller values of focus position are higher above the surface), only a single line is shown indicating the depth of the surface scribe. On the right side of the graphs, there are two lines showing the depths of the upper and lower bounds of the sub-surface modification. Where there are 3 data points at the same focus position, a multi-scribe exist.

With the 16x objective, there is a long range of focal positions where a surface scribe is cut due to larger depth of focus. There is no focal position where a multi-scribe feature is produced. With smaller NA of the 16x objective, the beam size is not large enough at the surface to go around the surface scribe line to create a sub-surface modification.

At a focus position of about 25 μm, the 20x objective produces both a surface scribe and inner modification at the same time. Multi-focusing and filamentation make the modification length longer.

With the 40x objective, only one focus position produced a clear surface scribe line since the depth of focus is so short. At a focus position of 25 μm, the sub-surface modification comes all the way up to the surface. If the surface scribe is too shallow, the sub-surface modification is too short, or the sub-surface modification is too close to the surface, a good cleave is more difficult to produce.

Figure 13 indicates that there is an optimum focusing condition for successful multi-scribe. The longer the focal volume above threshold, the longer and deeper inner modification is possible. With a larger NA there should be more energy which can go around the surface scribe for the same focus depth location although a large separation of the surface and inner scribe lines are more difficult because of the short focal volume.

Among the focusing conditions tested, the 20x aspheric lens produced the largest multi-scribe. The fastest speed which produced a successful cleave for a 100-μm thick wafer was 80 mm/s.

4. Laser Research System and Application Example

Fundamental laser research continues, to develop the next generation of ultrashort pulse fiber lasers. The same FCPA architecture has been used to construct research prototypes which extend the limits of pulse energy and average power [13,14]. One version of this fiber laser system produces 450-fs pulses with variable repetition rate from 100 kHz to 1 MHz at pulse energies of 5-10 μJ.

In parallel, select application studies are also being conducted to look for new processes enabled by this latest laser technology. One application of interest is high-speed laser surface texturing. This is particularly interesting because it allows for rapid modification of surface morphology over a wide area with a relatively modest average fluence of ~1 J/cm^2.

Despite the large bandgap energy and ablation threshold, surface texturing of sapphire can easily be achieved. SEM images show the resultant surface texture in Figure 14 for increasing accumulated laser fluence from 4.0 J/cm^2 to 0.45 kJ/cm^2, given an average single pulse fluence of 2.2 J/cm^2 at 500 kHz repetition rate.

The surface structures induced are self-organized into quasi-periodic ripples with a period ~1/3 of the 1040-nm laser wavelength. Similar Laser-Induced Periodic Surface Structures (LIPSS) are well known, and have been used in a variety of applications in which surface nano- and micro-

textures are used to modify the optical, chemical, and biological properties of materials [15-17].

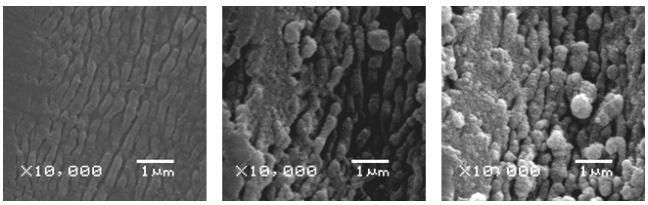

Fig. 14 Sapphire surfaces after ablation with accumulated fluences from 4.0 J/cm^2, ~2 pulses (left) to 0.45 kJ/cm^2, ~200 pulses (right).

Fig. 14 demonstrates that the degree of surface modification is highly dependent upon the accumulated laser fluence. Furthermore, by scanning a relatively small focal spot it is possible to texture a relatively large area and vary the accumulated laser fluence from point to point. We use this for a novel application, namely the fabrication of multilevel grayscale images; in a technique we call Femtosecond Laser Image Printing (FLIP). This technique has been used to fabricate an image of the Ginkakuji (Silver Pavilion) in Kyoto onto the surface of a 50-mm diameter sapphire wafer, as shown in Figure 15. The macroscopic appearance is the result of variations in light scattering based upon changes in the surface roughness. It takes 5 minutes to produce the 50 x 20 mm^2 image in Figure 15, corresponding to a processing speed of 2.0 cm^2/min.

Fig. 15 FLIP image of Ginkakuji (Silver Pavilion) in Kyoto machined onto sapphire surface.

5. Summary

The effect of repetition rates and pulse energy was tested for several micromachining examples with 10-μJ FCPA *μ-Jewel* D-1000.

Melting of fused silica (Corning 7980) and borosilicate (Schott D263) glasses were tested. Efficient thermal accumulation becomes possible even at lower repetition rates when the pulse energy is sufficiently high as long as ablation does not occur. Detailed thermal analysis has not been performed, but it is probably due to higher thermal diffusivity which is higher with fused silica.

The mechanisms behind previously demonstrated "dual scribe" process were investigated. Both shadowing and the nonlinear multi-focusing effect shape the inner modification.

The focus position for the onset of multi-scribe is slightly shallower in sapphire than in borosilicate glass due to the lower ablation threshold of sapphire (1.9 J/cm^2 for sapphire; 2.9 J/cm^2 for borosilicate glass [18,19]).

The surface scribe lines are necessary for initiating the break and the long inner material modification by multi-focusing helps to propagate the cleave facet in the direction perpendicular to the substrate surface.

With the multi-scribe method, a cleaner break is possible than with a single surface scribe line produced at the same speed.

Acknowledgments

The authors wish to thank Prof. Chris B. Schaffer for his useful discussion.

References

[1] B.C. Stuart, M.D. Feit, S. Herman, A.M. Rubenchik, B.W. Shore, and M.D. Perry: Phys. Rev. B, **53**, (1996) 1749.
[2] L. Shah, A.Y. Arai, S.M. Eaton, and P.R. Herman: Opt. Exp., **13**, (2005) 1999.
[3] K. Ke, E. F. Hasselbrink, Jr., and A. J. Hunt: Anal. Chem. **77** (2005) 5083.
[4] J. Bovatsek, A. Arai, and C.B. Schaffer: CLEO/QELS and PhAST Technical Digest (2006) CThEE6.
[5] S. Eaton, H. Zhang, P. Herman, F. Yoshino, L. Shah, J. Bovatsek, and A. Arai; Opt. Exp. **13** (2005) 4708.
[6] I. Miyamoto, A. Horn, J. Gottmann, D. Wortmann, and F. Yoshino: Journal of Laser Micro/Nanoengineering, **2** (2007) 57.
[7] R. Osellame, N. Chiodo, V. Maselli, A. Yin, M. Zavelani-Rossi, G. Cerullo, P. Laporta, L. Aiello, S. De Nicola, P. Ferraro, A. Finizio, and G. Pierattini: Opt. Exp. **13** (2005) 612.
[8] T. Tamaki, W. Watanabe, and K Itoh: Jpn. J. Appl. Phys. Part 2 **44**, (2005) L687-L689., T. Tamaki, W. Watanabe, and K. Itoh: Opt. Exp. **14** (2006) 10460.
[9] J. M. Bovatsek, A. Y. Arai, F. Yoshino, and Y. Uehara: Proc. SPIE, 6102, (2006) 610201
[10] F. Yoshino, J. M. Bovatsek, A. Arai, Y. Uehara, Z. Liu, and G. Cho: Journal of Laser Micro/Nanoengineering, **1** (2006) 258.
[11] Z. Wu, H. Jiang, L. Luo, H. Guo, H. Yang, and Q. Gong: Opt. Lett. **27** (2002) 448.
[12] J. B. Ashcom, R.R.Gattass, C. B. Schaffer, and E. Mazur: J. Opt. Soc. Am. B **23** (2005) 2317.
[13] L. Shah, M.E. Fermann, J.W. Dawson, and C.P.J. Barty: Opt. Exp. **14**, (2006) 12546.
[14] L. Shah and M.E. Fermann: IEEE Journal of Selected Topics in Quantum Electronics **13**, (2007), 522.
[15] A.Y. Vorobyev and C. Guo: Phys. Rev. B. **72** (2005) 195422.
[16] R. Younkin, J.E. Carey, E. Mazur, J.A. Levinson, and C.M. Friend: J. Appl. Phys. **93**, (2003) 2626.
[17] M. Groenendijk and J. Meijer: Journal of Laser Applicaitons **18**, (2006), 227.
[18] J. Bovatsek, L. Shah, A. Arai, and Y. Uehara: 5th Int. Symp. on Laser Precision Microfabrication, Proc. of SPIE Vol. 5662 (2004) p.661.
[19] J. M. Bovatsek, F. Yoshino, and A. Y. Arai: Proceedings of the 6th International Symposium on Laser Precision Microfabrication (LPM2005).

(Received: June 16, 2008, Accepted: November 12, 2008)